Microwave Electrothermal Propulsion for Space

John L. Power

Abstract—**The microwave electrothermal thruster (MET) is an attractive concept for medium or high power spacecraft propulsion. The heart of the concept lies in heating a propellant gas by passing it through a microwave plasma discharge. As described in the paper, the plasma is created in a resonant cavity by tuning either the TM(011) or the TM(012) mode for impedance-matched operation, using two internal tuning mechanisms. The MET concept is electrodeless, synergistically combines high pressure and high power capability, provides external control over the energy-conversion discharge, and operates on hydrogen propellant. Upwards of 95% efficiency has been reported in absorbing the applied microwave power in the plasma discharge. By employing a magnetic nozzle with the MET, substantial performance and life gains are expected due to reduced wall heating and losses, improved recovery of propellant internal energy, and discharge stabilization. Calculations of potential MET performance predict that 2000 sec. specific impulse at 6000 K average discharge chamber temperature and 1.0 MPa (10 atm.) pressure are reasonable goals with hydrogen propellant. Apparatus is described for testing the resonant-cavity MET to power levels of 30 kW at 915 MHz on nitrogen, helium, and hydrogen. It includes a superconducting magnet, providing field strengths to 5.7 T, to implement a magnetic nozzle. The low-ripple operation of the microwave generator has been verified, as has a procedure for starting the microwave discharge and raising the power applied to the cavity via a phase shifter-tuner. Impedance-matched resonant operation of the microwave cavity has been achieved.**

I. Introduction

FUTURE space missions of the National Aeronautics and Space Administration will require high performance thrusters not presently available [1]. Electric propulsion technology development over the past 30 or more years has incubated a number of promising propulsion concepts to fill this need. These may be categorized as either electrostatic, electromagnetic, or electrothermal. This paper presents one such promising concept in the electrothermal category which utilizes microwave power directly as the source of energy. The paper describes work in progress at the NASA-Lewis Research Center to test and develop this concept.

Electrothermal thrusters all operate on the principle of converting electrical or electromagnetic energy from an external source into thermal energy of a flowing propellant and then realizing this energy as thrust by expanding the heated propellant through a converging-diverging nozzle structure. The process is schematically depicted in Fig. 1. The input energy may be in the form of resistive heating of a heat transfer element, such as in the resistojet, or in the form of direct electric arc heating of the propellant, as in the arcjet. In other, electrodeless electrothermal propulsion concepts, the input energy is in the form of electromagnetic radiation. Radiation proposed or demonstrated as a feasible electrothermal thruster energy source includes low frequency rf radiation [2], high frequency laser radiation [3], and intermediate frequency microwave radiation. By means of suitable applicators, radiation of each type can be caused to create and couple strongly to a plasma discharge in a selected propellant gas, providing an energy conversion mechanism capable of handling high input power levels.

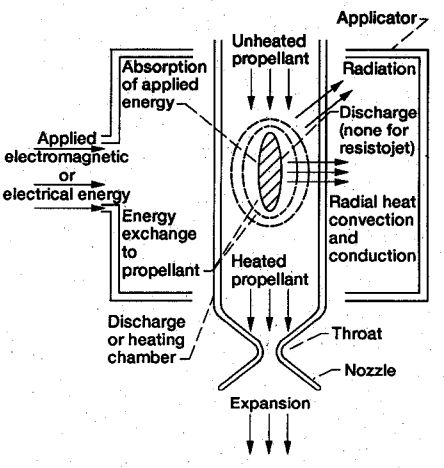

Fig. 1. Electrothermal Thruster Schematic.

As indicated in Fig. 1, several other processes are important in electrothermal thrusters following the initial energy absorption by the propellant. This energy must be efficiently converted into thermal energy of the exhausted propellant, which requires that the various loss mechanisms shown in the figure be minimized. Although much of the incident energy may be immediately converted into thermal energy, a major portion is also converted into internal energy of the propellant, in the form of excited, dissociated, and ionized species. This energy must be efficiently recovered as thermal energy of the propellant for the propulsion concept to be successful. As a result, careful attention must be paid to optimizing the thermal equilibration and relaxation processes which take place around and downstream of the energy absorption region.

The following section of this paper describes the microwave electrothermal propulsion concept, as imple-

Manuscript received June 5, 1991; revised January 29, 1992.

The author is with the Space Propulsion Technology Division, NASA Lewis Research Center, 21000 Brookpark Road, MS SPTD-1, Cleveland, OH 44135.

mented with a resonant cavity applicator, and treats various aspects of it including its potential performance, how energy losses in it may be minimized, integrating it with a magnetic nozzle, and operating it at high power levels. Section III then presents the experimental apparatus in final assembly at the NASA-Lewis Research Center to test the concept at relatively high power, describes the diagnostics to be employed in this evaluation, gives preliminary results from testing components of the apparatus, and outlines the planned testing sequence.

II. The Microwave Electrothermal Thruster Concept

A. Description

The microwave electrothermal thruster (MET) employs continuous wave microwave energy to create and maintain a plasma discharge in a flowing propellant gas. The discharge then acts to absorb the applied microwave energy and transform it into thermal and internal energy of the propellant. Expansion and expulsion of the hot propellant through a throat and nozzle finally convert the energy of the gas into thrust. The success of the MET concept requires high efficiencies in all these processes. For interest as an advanced propulsion concept, the energy conversion process must also permit high energy densities in the discharge volume and be compatible with the use of the highest performance propellant gases, namely, hydrogen or gas mixtures consisting largely of hydrogen.

The microwave absorption process requires an applicator through which the propellant gas passes while being confined in a discharge tube or chamber, as seen in Fig. 1. Three types of applicators have been successfully investigated to date: the resonant cavity [4], the coaxial applicator [5], and the waveguide applicator [6]. Only the resonant cavity is considered in this paper. In such a cavity applicator, three requirements must be met. First, a single mode must be selectively excited and all others excluded, in order to concentrate all the incident microwave energy absorption in a single volume element suitably located within the flowing propellant. Second, this energy absorption volume must be located on the axis of the cavity to facilitate its placement within the propellant stream and to separate it as far as practicable from the cavity walls. Third, the cavity must be provided with tuning mechanisms permitting exact frequency and impedance matching of the cavity mode and load with the external circuit supplying the microwave power.

Two low-lying cavity modes, the TM(011) and the TM(012) modes, allow meeting the above requirements. The standing electric and magnetic field patterns of these transverse magnetic modes in a cavity are depicted in Fig. 2. Both can be exclusively excited and both concentrate the strongest electric fields on the cavity axis, the TM(011) near the cavity endwalls and the TM(012) at the midplane. Since the strongest electric fields define the plasma discharge region, both modes are candidates for the MET. The TM(011) mode has two potential advantages in that, firstly, it places the discharge volume close to the end of the cavity, so that an external throat-nozzle assembly may be located close to the energy absorption region, and, secondly, the cavity need be only half as long as for the TM(012) mode.

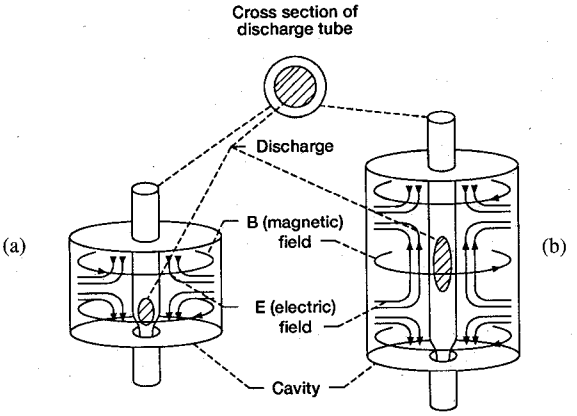

Fig. 2. MET Cavity Modes. (a) TM_{011}. (b) TM_{012}.

As shown, for example, by Frasch [7], two independent tuning mechanisms are necessary to exactly match the complex impedance of the cavity, with its load, to the microwave source circuit. Integrating the tuning mechanisms as part of the cavity itself is desirable to avoid separate power losses in them. By making one of the cavity endwalls movable and the power input antenna insertion into the cavity adjustable, the needed tuning capabilities can be readily achieved.

The coupling of the microwave energy in the cavity electromagnetic fields to the propellant occurs primarily by the acceleration of free electrons in the gas plasma by the strong, standing electric field present in the discharge region. The accelerated electrons transfer their absorbed energy by collisions with the ions, atoms, and molecules present, causing further heating, ionization, and excitation of these species, plus the production of more free electrons. This process is enhanced at higher pressures, where collisional frequencies are higher and mean free paths shorter. So long as the input microwave power absorbed is kept high enough to prevent the discharge plasma from being quenched by the cold neutral species present, the pressure may be raised to high levels, well over atmospheric [8]. In this pressure regime, the plasma approaches a condition of local thermodynamic equilibrium, with all the microwave power input to each free electron converted within microscopic dimensions into internal and kinetic energy of all the charged and neutral species present.

A good measure of the microwave energy absorption efficiency achievable in a resonant-cavity MET is provided by comparison of the Q (quality) factor of the empty versus the plasma-loaded cavity. The empty cavity Q factor is reduced from a value approaching 15000 [7] to a value of 20–120 [9] with a low power discharge. These values correspond to efficiencies of 97.5 to 99.7% in the

absorption of the microwave energy by the plasma discharge.

Once the microwave energy has been absorbed in the MET discharge, it must be efficiently converted and extracted as kinetic energy of the exhausted propellant. The principal energy loss mechanisms in this process are in 1) heating of the discharge chamber and cavity walls by radiation, conduction, and convection from the hot plasma and 2) frozen flow losses in the expelled propellant. The latter refer to the energy losses incurred when dissociated, excited, or ionized propellant species exit the nozzle without having relaxed to the corresponding ground-state molecular species, thereby carrying off dissociation, excitation, or ionization energy unconverted to the desired kinetic energy. Minimizing these energy losses is discussed below.

Both the incident microwave power and the discharge chamber pressure are important control parameters in the operation of the MET. The power is directly controlled, but the pressure can only be indirectly adjusted by such other variables as the propellant flowrate. Increasing the power increases the energy absorption and discharge volumes. Increasing the pressure in the discharge zone, other parameters being unchanged, decreases the discharge volume because of the increased collisional frequencies and decreased mean free paths. These opposing effects can be utilized to maintain the discharge volume approximately constant as the applied power is changed, a very useful capability which suggests that the MET promises excellent throttling characteristics. Starting the MET at low power and then raising the power to the desired operating level is also facilitated.

The MET concept derives a major advantage over other electric propulsion devices in which DC arcs pass through the propellant or in which the propellant is conductively heated from the fact that it does not require any contact of electrodes, heating elements, or other structures with the hottest propellant. Thereby the major life- and performance-limiting processes which such contact causes in arcjets, resistojets, and related thrusters are totally avoided in the MET.

The choice of the microwave frequency employed in the MET depends on several considerations. The microwave energy conversion process described above is efficient over a wide frequency range and does not pose a major limitation. However, the dimensions of the resonant cavity, as well as of waveguide and coaxial transmission lines, scale with the wavelength of the microwave radiation. For practical purposes this limits the choice to the industrial heating frequencies of 915 and 2450 MHz, the corresponding wavelengths of which are 33 and 12 cm, respectively. Although investigation of the MET concept to date has been exclusively with radiation of the higher frequency, use of the lower frequency offers several advantages. The larger size of the cavity, discharge chamber, and throat/nozzle assembly for the 915 MHz radiation simplifies fabrication and facilitates observation of their operation. Other advantages lie in the higher efficiency and much lower cost of magnetron generators for the lower frequency radiation, both of which are major factors in the realization of a high power MET. The major disadvantage of employing the lower frequency is that the cavity, transmission lines, and generator are bulkier. Based on these tradeoffs, the 915 MHz frequency was selected for the investigation here reported.

B. Potential Performance

The propulsion performance capabilities of the MET concept have been predicted with hydrogen as the propellant [10] by the use of an industry-standard two-dimensional kinetics (TDK) computer code [11]. This code has been extended to include high temperature reactions involving ions, electrons, and third bodies. The computations incorporate thermodynamic and kinetic data up to 20 000 K for all the species and reactions of the hydrogen system. As explained below, thruster performance is computed under different assumptions by four modules of the code, which are named: one-dimensional equilibrium (ODE), one-dimensional frozen flow (ODF), one-dimensional kinetics (ODK), and two-dimensional kinetics (TDK).

The code first calculates the equilibrium conditions in the reaction or discharge chamber, for a given specification of the chamber pressure and temperature or enthalpy. Then it computes the local conditions and engine performance as the discharge chamber mixture expands through the geometrically specified converging and diverging sections of the throat/nozzle configuration. The expansion calculations are done in one dimension under separate assumptions that: 1) local thermodynamic equilibrium is maintained throughout the whole process (ODE); 2) frozen flow is maintained throughout the whole process (ODF), in which case the equilibrium concentrations computed for the discharge chamber are held fixed throughout the expansion; and 3) the local concentrations at each point in the expansion are determined by the specified reaction kinetics (ODK). Finally, a full two-dimensional computation (TDK) of the local conditions and engine performance is done under assumption 3).

Perhaps the most important engine performance parameter calculated by the TDK code is the specific impulse (Isp), which gives the thrust produced per unit mass of propellant consumed per second. Fig. 3 shows the Isp calculated by the four modules of the code for a MET operating on hydrogen, as a function of the mass-averaged propellant temperature in the discharge chamber. A constant discharge chamber pressure of 1.01 MPa (10 atm.) and a constant input enthalpy (absorbed power) of 107 kW are assumed in all the computations. The calculations are for a simple converging/diverging nozzle configuration having a 2 mm diam. throat, a 25 degree contraction angle, a 15 degree expansion angle, and a nozzle exit area ratio (relative to the throat area) of 75. (This throat/nozzle configuration is closely realized in the experimental apparatus discussed in Section III.) The results shown in

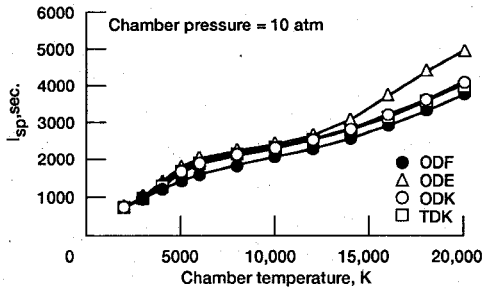

Fig. 3. MET Predicted Performance.

Fig. 3 are typical of the TDK calculations. The Isp's calculated by ODE are always the highest because the chemical equilibrium assumption results in the greatest recovery, as kinetic energy, of the dissociation, excitation, and ionization energy injected into the propellant by the microwave energy conversion process. The Isp's calculated by ODF are always the lowest because none of this energy is recovered. The ODK results are intermediate between the ODF and ODE computations because they account for the finite kinetics of the reactions which recover the internal energy of the propellant species. The TDK results, which are the most realistic of all, are slightly lower than the ODK results because they take into account edge and wall geometrical effects.

The Fig. 3 results provide important predictions of the MET's potential performance on hydrogen propellant. It is seen from the TDK curve that an Isp of about 2000 sec. can be achieved for an average discharge chamber temperature of 6000 K, and that not much improvement in the Isp is realized if the chamber temperature is raised as high as 12 000 K. This is because the propellant is largely in the form of atomic hydrogen, and the exhaust temperatures and pressures in the nozzle are such as to permit recovery, even under equilibrium conditions, of only a decreasing portion of the dissociation energy invested in the propellant over the indicated temperature range. As a result, it is clear that an average discharge chamber temperature of about 6000 K should be a goal for MET operation of hydrogen and that operation at Isp's substantially above 2000 sec. is not feasible with conventional converging/diverging nozzle configurations, such as that specified for the TDK calculations.

Achieving an average chamber temperature of 6000 K is a challenging but feasible objective. Electron temperatures as high as 13 000 K have been reported in high pressure microwave discharges [12]. To attain a 6000 K average temperature requires just such a hot plasma core volume, surrounded by progressively cooler gas having a radial temperature profile such that the temperature at the wall is down to material thermal limits of about 2200 K.

A second observation from Fig. 3 is that the TDK results are close to the limiting ODE results at temperatures up to about 12 000 K. This implies that the kinetics of the recombination and relaxation processes in the hot hydrogen propellant are fast enough and the nozzle pressures high enough that the frozen flow losses are low up to this temperature. Above about 12 000 K, thermal ionization of the now almost completely atomic hydrogen propellant becomes important, and, as seen in Fig. 3, the TDK curve diverges from the ODE calculations to closely follow the ODF results. This indicates that the ionization energy invested in the propellant in this temperature regime is only poorly recovered in the expansion process and that the frozen flow losses become substantial. It suggests that it is undesirable to operate the MET at conditions generating high levels of ionization in the discharge plasma because of the frozen flow losses incurred due to the remanent ionization of the propellant exhausted from the nozzle.

The thrust predicted for the MET in the TDK calculations was found to be strictly proportional to the discharge chamber pressure, in accord with theory [10]. A thrust of 6.04 N and a hydrogen flowrate of 0.326 g/sec. were calculated for a 6000 K chamber temperature at the assumed chamber conditions of 1.01 MPa (10 atm.) pressure and 107 kW absorbed power. The theoretical thermal efficiency calculated for these conditions is 52%.

C. Minimizing Losses

The TDK calculations of predicted MET performance discussed in the previous section neglect plasma-wall interactions, other boundary layer effects, and radiative heat losses, all of which reduce the thruster performance by decreasing the thermal efficiency. The resonant-cavity MET concept provides considerable flexibility in designing and operating the thruster to minimize these losses. This is principally because the plasma discharge is not fixed in location relative to the physical structure of the discharge chamber, nor is it attached to any part of this structure. Furthermore, the plasma discharge volume and, to some extent, shape are also not fixed and may be altered by externally controlled variables. Mentioned already are the opposing effects of the discharge chamber pressure and absorbed microwave power on the discharge volume. Other externally controlled variables influencing the size, shape, and location of the discharge volume include the characteristics of the gas flow into and around it (including swirling flow and radial variation of the injected flow distribution), magnetic fields, and gravity. The beneficial effects of magnetic fields are discussed in the following section. The effect of gravity is to exert buoyancy forces on the discharge volume because of its lower density than the surrounding colder gas. The goal in designing and operating the MET is to control the above variables to place and confine the discharge volume within the discharge chamber so as to maximize the bulk average temperature of the propellant as it passes into the throat while minimizing the thermal losses to the structure.

Few attempts have been made to date to optimize the MET design and operation for maximum performance and thermal efficiency. One desirable design objective in accomplishing this is to assure that the discharge chamber, throat, and nozzle all operate at the highest feasible tem-

peratures, because the maximum thermal efficiency is achieved if these components operate uncooled. This requires minimizing the thermal losses from them to the external environment by incorporating such features as a vacuum jacket around the components, low emittance surfaces on their exterior, and highly reflective finishes on the external surfaces thermally irradiated by them.

Materials considerations are also important for the discharge chamber, throat, and nozzle. Not only must these components be fabricated of materials tolerating the highest possible operating temperatures, but the materials employed inside the cavity must have maximum transparency to the microwave radiation in use in order to minimize the microwave power absorption and heating in them. Several materials exist, including boron nitride and alumina, which combine structural strength, high temperature capability, and a low dielectric loss tangent to make them excellent candidates for the in-cavity components.

Thermal efficiencies of almost 50% have been measured [13] in resonant cavity MET operation on nitrogen. Efficiencies as high as 80% have been reported by Haraburda and Hawley [14] in converting incident microwave power into thermal energy of nitrogen propellant in other resonant-cavity MET experiments, though most of the thermal energy was removed by cooling the discharge tube rather than as kinetic energy of the exhausted propellant. With minimization of the thermal losses in the MET, performance approaching that predicted by the TDK computations shown in Fig. 3 is potentially realizable.

D. Magnetic Nozzle

An attractive means for improving the performance, thermal efficiency, and operation of the resonant-cavity MET lies in implementing a so-called magnetic nozzle with it. The concept is illustrated in Fig. 4, as depicted with the TM(011) mode excited in the cavity. A strong DC solenoidal magnetic field, aligned coaxially with the cavity and situated adjacent to it, creates the magnetic nozzle. Unlike its use in magnetoplasmadynamic (MPD) and electron cyclotron resonance (ECR) thrusters, the magnetic nozzle is not employed in the MET for electromagnetic acceleration of the propellant to produce thrust. Instead, due to the action of the plasma in excluding the field lines, the field acts to strongly constrain and control the plasma discharge in the MET cavity, as well as the residual plasma in the heated propellant as it flows downstream through the thermalization, contraction, and expansion regions of the throat and nozzle. The magnetic field exerts a strong pinching force on the plasma by restricting the cyclotron radii of the ionized species present, thereby creating a radially inward-directed pressure on the plasma which must be balanced by an increase in the plasma kinetic pressure. This process acts to compress the plasma along the common axis of the cavity, discharge chamber/throat/nozzle assembly, and magnet, thus increasing the plasma density and collision frequencies and reducing the plasma volume. The field also creates a force

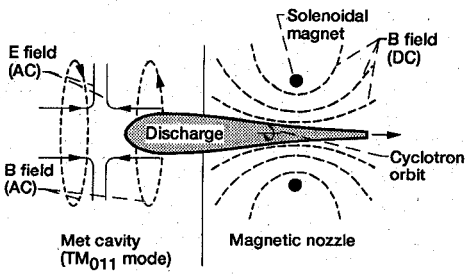

Fig. 4. Magnetic Nozzle with Resonant Cavity MET.

component repelling the plasma discharge, tending to push it upstream.

The magnitude of the magnetic pressure created in a magnetic nozzle is proportional to the square of the magnetic field strength. With modern superconducting magnets these pressures can be quite high: 0.4 MPa (4 atm.) at a 1 T field strength and 14 MPa (140 atm.) at a 6 T field strength. With a kinetic pressure of up to 1.0 MPa (10 atm.) in the MET discharge chamber during operation, the magnetic pressure created by the magnetic nozzle may readily predominate.

Several important benefits accrue from the use of a magnetic nozzle with the resonant-cavity MET. The hot plasma is compressed away fron the confining walls of the discharge chamber, as well as those of the throat/nozzle assembly, thereby reducing the plasma-wall interactions, heating, and consequent thermal losses. Conversely, the magnetic field strength can be controlled to adjust the plasma discharge diameter relative to that of the discharge chamber for optimum performance. Furthermore, the reduced plasma volume and increased plasma density and pressure within the magnetic nozzle promote the recombination and third body reactions which recover the ionization and excitation energy of the plasma species as thermal energy, due to the effects of these parameters on the reaction equilibria. A final benefit lies in the field's effect of stabilizing and fixing the discharge volume exactly on the system axis. This prevents destabilizing effects such as flow inhomogeneities or buoyancy forces from causing displacement of the discharge from its optimal location (and possibly disastrous contact with the discharge chamber wall).

A critical region wherein the magnetic nozzle plays a crucial role is the throat. Here the wall heating by the hot residual plasma present often is the most intense, but here too the field strength from the magnetic nozzle can be adjusted to be the highest, so that the constriction of the plasma matches the constriction of the gas flow by the walls. This effect may considerably ameliorate the critical life- and performance-limiting problem of throat overheating, which commonly constrains uncooled thermal rocket engine operation. The cyclotron radii of 10 000 K protons and electrons in a 6 T magnetic field are 2.7×10^{-2} and 6.0×10^{-4} mm, respectively, so that confinement of these species away from the wall is feasible even in a 2 mm diameter throat.

E. High Power Operation

As a useful propulsion device for a wide range of potential applications from orbit raising to interplanetary travel, the MET must be developed to operate at power levels of 30–100 kW or higher, with a thrust of at least 1.8 N and a specific impulse of at least 1500 sec. These power levels are an order of magnitude higher than in any MET operation investigated to date. At such power levels additional concerns arise. These are considered in this section.

As the applied power level and the power density in the plasma discharge volume are increased after starting the MET, the electron density in the plasma also increases, typically to values above $10^{12}/\text{cm}^3$. At 915 MHz, the plasma frequency electron number density is $1.0 \times 10^{10}/\text{cm}^3$. As the plasma density exceeds this level, the standing electric fields of the cavity mode in use, which are responsible for coupling the microwave power to the free electrons of the plasma, penetrate less deeply into the plasma volume. At some relatively high level of power density in the plasma, this skin effect excludes the impressed electric fields from all but the outer sheath of the plasma.

Above the skin effect plasma density limit, the plasma kinetic pressure is so high that increasing the gas pressure in the discharge chamber is no longer effective in reducing the plasma volume. Any further increase in the absorbed microwave power simply expands the plasma volume without significantly increasing its power density, regardless of pressure increases. This power density limit in the plasma, together with the available discharge chamber cross-sectional area, then limits the power level at which the MET can be operated. Otherwise stated, for high power operation the discharge chamber must be so sized that the plasma cross-sectional area yields optimal performance at the desired power level. It is then not possible to operate the thruster optimally over a range of power levels, in contrast with the ability under low power operation to adjust the pressure along with the power to maintain optimal plasma dimensions as the power is varied.

The one operational control parameter which still may be effective after the skin-effect power density limit has been reached is the magnetic pressure exerted by the magnetic nozzle. If this pressure is sufficiently great, it may still afford some capability to optimize the plasma size and increase the electron and power densities above the normal skin effect limits.

The skin effect limitation on the absorbed power density in the discharge volume affords two quite important advantages which may favor operation and optimal performance of the MET under such conditions. The first of these is that with absorption of all the applied power in a thin outer sheath of the plasma, the desired equilibration and heat exchange of the hot plasma with the surrounding colder propellant gas is facilitated. The energy absorption takes place exactly where the energy interchange is required. The second advantage is that little of the incident energy is then directly absorbed in the hottest central zone of the plasma, effectively flattening the temperature profile across the plasma volume and thus minimizing thermal radiation losses from it.

A final ramification of high power MET operation is the necessity of a low ripple ($< \sim 2\%$, peak-to-peak), narrow bandwidth output signal from the microwave generator. Without this, the plasma-loaded cavity can only be approximately matched in impedance to the microwave source, with no tuning at all possible for the ripple component of the signal. At the high power levels of interest, even small source-load mismatches result in substantial reflected power losses which must be accommodated in and therefore complicate the microwave circuit.

III. Status of Experimental Work

A. 30 kW Test Apparatus

This section presents a summary description of the apparatus being set up [10] at the NASA-Lewis Research Center to test the resonant cavity MET concept at power levels to 30 kW. As of the writing of this paper (May, 1991), assembly of this apparatus is nearing completion. The components of the experimental system are discussed in the following order: the microwave generator, the microwave circuit, the cavity, the discharge tube system, the magnetic nozzle, the throat/nozzle structure, and the vacuum facility.

1. Microwave Generator: The microwave generator employed is a magnetron-type industrial heating unit specially modified to produce a low ripple output signal. The CW output power is adjustable from about 2 to nominally 30 kW (in 3 ranges) and the output frequency varies from 911 MHz at low power levels to 916 MHz at the higher levels. The basic 915 MHz frequency was selected because of the considerations discussed in Section II-A. The output signal bandwidth is typically 0.2 MHz, and the signal contains no significant sideband radiation. The generator is designed for a system impedance of 50 Ω. The magnetron tube of the generator is protected from excessive reflected radiation by a 3-port circulator. In addition, a sensor is installed in the output waveguide which senses the reflected power reaching the generator, displays it, and shuts off the output power if the reflected power exceeds 10 kW.

In order to meet the $(\pm)1\%$ specification on the peak-to-peak ripple of the output signal at full power, a dual secondary, 3-phase plate transformer with a full-wave rectified output circuit is employed in the generator. Additional modifications and considerable filtering are also incorporated in the magnetron anode and heater circuits to reduce the ripple. To further minimize it, the generator is powered from a 440 VAC line regulator in which the three phase voltages are independently balanced. Measurements made of the output ripple with all of these provisions in place are represented in subsection C below.

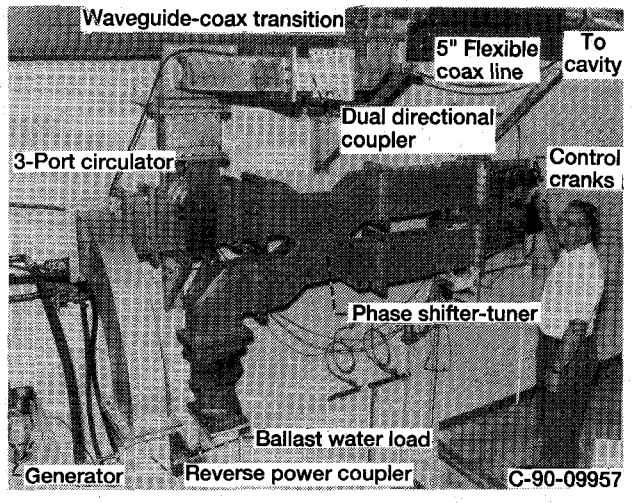

Fig. 5. MET Apparatus Microwave Circuit.

2. Microwave Circuit: Fig. 5 depicts most of the microwave circuit between the generator and the cavity. The waveguide portions of the circuit are constructed of standard WR975 waveguide. From the generator this leads through the reflected power directional coupler and a 3-port circulator (distinct from the one in the generator) to a large phase shifter-tuner unit. This contains two double-bucket shorting assemblies which may be manually positioned by external cranks to achieve up to a 400 degree phase shift in the signal and reflect any portion of it (up to a nominal 98%) back into the 3-port circulator. That portion of the input signal not reflected passes through the output port to a ballast water load, where it is fully absorbed. The water load is rated to accept the full output power of the generator.

The portion of the signal reflected back into the circulator is fully diverted (with 23 dB isolation) into the upward directed leg seen in Fig. 5, from which it passes through a dual directional coupler (providing measurements of the forward and reverse power levels in this leg) to a waveguide-to-coaxial line transition. From here to the microwave cavity the signal passes through approximately a 5 m long section of 12.7 cm (5 in.) diameter flexible coaxial transmission line. The coaxial line is rated under laboratory conditions for about 32 kW of CW microwave power at 915 MHz, attenuates the signal by less than 0.05 dB, and has a cutoff frequency of about 960 MHz.

The use of the phase shifter-tuner to control the power directed to the cavity is necessary because the magnetron generator does not allow direct adjustment of the output power from low levels of perhaps 250 W, suitable for starting a discharge in the cavity, up to substantial operating levels. Instead, the generator will be operated at a constant power level, somewhat above the maximum applied power level required in the cavity. The phase shifter-tuner will first be adjusted for no power reflection to the cavity, then readjusted to apply the starting level of power, and finally, after the discharge is started, will be further adjusted as required to continuously raise the applied power to the operating level. During the last step, it will also provide an additional tuning means which may be used in conjunction with both cavity tuning adjustments to maintain the circuit optimally tuned for minimum impedance mismatch. Maintaining the generator at a fixed, higher output level via this operating strategy has the significant benefits of improving the stability of the output signal and avoiding the frequency shift associated with changing the magnetron output power. Results from testing this operating strategy with a water load simulating the cavity load are presented in subsection C below.

3. Cavity: Fig. 6 shows the resonant cavity with its front flange opened to expose all the interior surfaces. The cavity is a cylinder 45.7 cm in inside diameter by 57.2 cm long. The front end flange is fixed, but the rear end flange is manually movable by a gearing assembly which maintains the flange surface perpendicular to the cylindrical wall. This provides one of the two required internal tuning mechanisms for the cavity. Fingerstock mounted on the outside circumference of the movable shorting flange maintains it always in good electrical contact with the cylindrical surface. The shorting flange may be translated over a distance of 24.1 cm, allowing the interior length of the cavity to be adjusted from 16.5 to 40.6 cm. This covers the calculated lengths of 19.6 and 39.2 cm, respectively, anticipated for tuning the TM(011) and TM(012) modes at 915 MHz. A few other, mostly TE, modes are also expected to be tunable at this frequency within the available shorting flange travel.

The power input port of the cavity is seen prominently in Fig. 6 with its center conductor probe, which acts as the input antenna. This port is centered at a distance of 9.8 cm from the inside front flange surface of the cavity. This is the expected location of the downstream electric field maximum of the TM(011) mode, so placement of the input power port here should facilitate coupling of the incident microwave signal to this mode. The power input probe insertion into the cavity is adjustable over a 3.6 cm range by a captivated threaded ring which is part of the input port assembly. This provides the second internal tuning mechanism for the cavity. The coax line which transmits the power from the microwave circuit mates with the power input port via standard EIA 15.6 cm (6 1/8 in.) connectors. The figure shows these connectors, but instead of connecting to the coax line they are seen connecting to a reducer and adapter which enable sweep generator testing of the cavity at low power.

As seen in Fig. 6, the cavity has a 6.3 × 6.3 cm viewport, protected by 0.64 cm machined mesh screening, located under the power input port. This will provide direct observation of the TM(011) mode discharge plasma. In the movable shorting flange at the upstream end of the cavity, a 73 mm diameter hole centered on the axis provides clearance for the vacuum liner which encloses the discharge tube, both of which extend through the entire cavity. In the fixed downstream flange a 70 mm hole centered on the axis provides an O-ring vacuum seal to the vacuum liner.

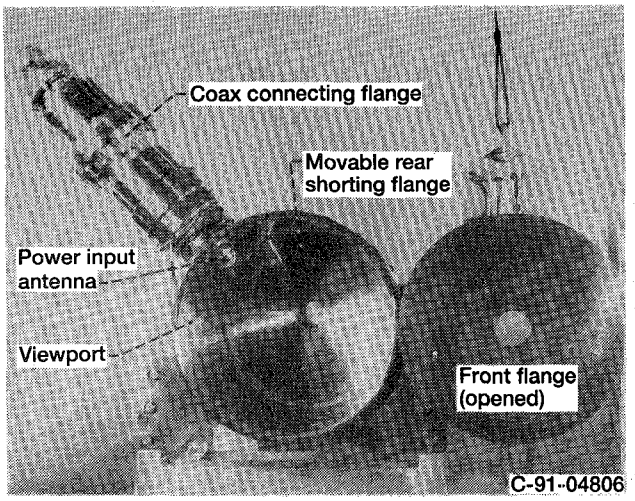

Fig. 6. Microwave Cavity for MET Testing.

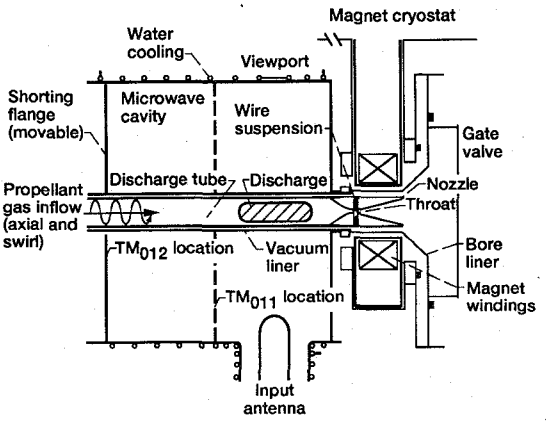

Fig. 7. MET and Superconducting Magnet Apparatus Configuration.

The cavity is entirely fabricated of OFHC copper. All its interior surfaces, including those of the power input port, are silver-plated to a thickness of up to 0.08 mm, and the plated surfaces are polished to be as reflective as possible. The silver plating and polishing are intended not only to minimize surface current losses but also to reflect the maximum amount of thermal radiation incident on them back to the discharge tube. All of the cavity walls, as well as the power input port, are water-cooled on their exterior surfaces. The total cooling capacity of these water cooling loops is substantially greater than the 30 kW maximum power output of the microwave generator. Each loop is instrumented with a flowmeter and immersed thermistors to implement calorimetry measurements.

4. Discharge Tube System: Fig. 7 shows the configuration of the assembled cavity, discharge tube and vacuum liner, magnetic nozzle magnet, throat/nozzle structure, and vacuum facility gate valve in the MET test apparatus. The discharge tube and vacuum liner, together with the propellant gas injector at the upstream end of the discharge tube, comprise the discharge tube system and are aligned on the cavity axis. As noted in Section II, the purpose of the vacuum liner is to provide a vacuum barrier completely surrounding the hot discharge tube to minimize conductive and convective heat losses from the latter.

For initial low power testing, a transparent fused quartz discharge tube will be employed to enable direct observation of the plasma discharge inside. The inside diameter of the tube is 50 mm and its wall thickness is 2.5 mm. Besides being transparent to visible light, the fused quartz is also quite transparent to microwave fields, as evidenced by its low dielectric loss tangent. It has good strength, but its maximum service temperature is limited to about 1750 K. This will restrict testing with it to modest microwave power levels. For subsequent testing at high power levels, it is expected that discharge tubes fabricated of alumina or boron nitride will be employed. Both materials have good strength at high temperatures, and their operating temperature limits are above 2200 K in non-reactive environments. They are also quite transparent to microwave fields at 915 MHz but are opaque to visible light, so that direct observation of plasma discharges inside tubes of them will be impossible. Discharge tubes of all of the above materials are expected to withstand discharge chamber operating pressures of up to 1.0 MPa (10 atm.) if their material service temperature limits are not exceeded.

The vacuum liner is also fabricated of fused quartz. Its outside diameter of 69.5 mm and wall thickness of 2.3 mm provide an evacuated annulus about 5 mm thick around the quartz discharge tube. The optical transparency of the vacuum liner, besides permitting direct observation of the plasma discharge in the initial quartz discharge tube tests, will be important in the later higher power testing with opaque discharge tubes, because it will allow some characterization of the discharge region by the visible and infrared radiation from the hot discharge tube walls.

The propellant gas injector in the upstream end of the discharge tube is designed to provide two propellant gas inflow streams, one directed axially along the tube axis and the other directed tangentially along the tube wall. The latter stream provides a swirl flow component which has been found important [15] in stabilizing the arc discharge plasma in arcjets and which is expected to be especially effective in stabilizing the plasma discharge during MET operation. Each of the two propellant gas streams from the injector is supplied and controlled by an independent feed system which can provide up to 25 000 sccm flow at discharge chamber pressures up to 1.0 MPa (10 atm.). Pure nitrogen, helium, and hydrogen will be investigated as the propellant gases in the initial MET testing.

5. Magnetic Nozzle: The magnetic nozzle for the MET testing is formed by the superconducting magnet indicated in Fig. 7, which is mounted coaxially with and immediately downstream of the microwave cavity. The magnet is a short solenoid, having a length of about 81 mm and a through-bore of 89 mm, measured as the dimensions of the liquid nitrogen (LN2)-cooled shield and

bore liner. The magnet is provided with flanges from which a water-cooled room temperature bore liner of 70 mm inside diameter is mounted. This room temperature bore liner, made of OFHC copper, has a reflective interior finish and is designed for a thermal loading of at least 25 kW. At its downstream end it conically expands to accommodate the exhaust plume expansion from the MET nozzle. Because the magnet windings must be submerged in liquid helium (LHe) from a reservoir situated above them and all the LHe-cooled components must be shielded by LN2-cooled surfaces, with the LN2 supplied by another reservoir located above the magnet, the magnet bore and hence the MET apparatus is constrained to a horizontal orientation. All LHe- and LN2-cooled surfaces in the magnet assembly are vacuum shielded to minimize heat leakage and cryogen usage.

The maximum on-axis magnetic field strength generated by the NbTi magnet windings, on the mid-plane of the magnet, is 5.7 T. Higher field strengths, up to 7.8 T in the magnet windings themselves, are generated at increasing radial distances from the axis, so that a positive radial field gradient exists at essentially all radial and axial locations within the magnet bore.

The magnet power supply allows ramping the winding current up or down at any constant rate up to 15 A/min. to any final current values up to the maximum of 117 A. This high ramping rate is enabled by the relatively low magnet winding inductance of 7.9 H. The field strength is linear with the winding current, demonstrating negligible hysteresis; hence, the magnet current accurately specifies the field strength. The magnetic field polarity may be automatically reversed, requiring about 16 min. when the magnet is at maximum field strength.

A switch is incorporated in the magnet which enables persistent mode operation of the magnet at any fixed current and field strength up to the maximum. During such operation the magnet power supply is effectively disconnected from the winding circuit, minimizing cryogen consumption. Negligible decay (less than one part in 10^5 per hour) of the magnet field strength and current is observed over periods of days in this mode of operation. The magnet also is designed and has been tested to withstand quenching during full field operation without damage.

6. Throat/Nozzle Structure: The throat/nozzle structure of the MET test apparatus, as seen in Fig. 7, is attached to the downstream end of the discharge tube by a high temperature mechanical seal. Its geometrical design closely duplicates the configuration used for the TDK performance calculations described in Section II-B, except for having a 1 mm diameter throat instead of the 2 mm throat in the calculations. The smaller throat is necessary to achieve the desired discharge chamber pressures at the available experimental power levels and propellant flowrates.

The throat/nozzle structure, as well as the attached discharge tube, is suspended in position on the common cavity/magnet axis by a refractory metal wire attached to a support frame which fits inside the water-cooled magnet bore liner. This arrangement minimizes the heat lost from the throat/nozzle by conduction to the cooled support structure. It also permits positioning the throat at any of several axial locations with the magnet bore. This enables investigation of the magnetic nozzle operation and efficacy with the throat positioned 1) in the converging magnetic field upstream of the magnetic field maximum, 2) at the field maximum, or 3) in the diverging field downstream of the field maximum. Optimum performance is expected with the throat located near or at the field maximum.

The throat/nozzle structure is designed as a relatively massive, one-piece, refractory metal fabrication. Its massiveness is intended to bring it to a constant temperature during steady state operation under fixed conditions. This temperature will be measured, as described below, and will provide a sensitive indication of the magnetic nozzle's effectiveness in controlling wall heating in the throat and nozzle by the hot propellant from the discharge chamber.

7. Vacuum Facility: The hot propellant exhaust from the nozzle of the MET apparatus expands through a 30 cm diameter gate valve, indicated in Fig. 7, into a 3.0 m diameter by 5.8 m long vacuum tank [16]. The gate valve is on the side of the tank and directs the MET exhaust against a LN2-cooled cryoliner mounted from the interior wall on the opposite side of the tank. The cooling capacity of this cryoliner is well in excess of the 30 kW maximum output power of the microwave generator. The cooled exhaust gas is evacuated by the tank's six large diffusion pumps, blower, and two mechanical pumps. The tank vacuum also serves to pump the vacuum annulus in the vacuum liner surrounding the discharge tube. Tests measuring the vacuum facility's pumping capacity for nitrogen, helium, and hydrogen, the three propellant gases to be investigated, have been conducted. The results are reported in subsection C below.

B. Diagnostics

The initially deployed diagnostics for the MET experimentation are rather rudimentary. The measurements acquired are intended to characterize basic thruster performance, thermal losses, and magnetic nozzle effects.

Water calorimetry is extensively employed in the MET testing to measure microwave power levels and determine thermal losses. The measurements are simply taken by reading a water flowrate for a given cooling loop or microwave water load and the temperature rise due to the thermal loading of the coolant, as given by immersed thermistors. Except for the microwave generator water circuit, all cooling loops in the apparatus are calorimetrically instrumented. These include the cooling loops for the external 3-port circulator and the ballast water load, six cooling loops on the walls of the cavity, one loop on the upstream end of the discharge tube system, two loops on the magnet bore liner, and one loop on the vacuum tank gate valve and its mounting spoolpiece. The LN2-

cooled cryoliner in the vacuum tank, which acts as the target and heat exchanger for the propellant exhausted from the MET, also is to be instrumented for rough calorimetry of the beam power.

With the phase shifter-tuner adjusted so no power is applied to the cavity, calorimetric measurements made on the ballast water load accurately give the output power level of the microwave generator, which normally will be maintained unchanged during an experiment. With power applied to the cavity, the ballast water load power is again measured. This power, plus the reflected power read from the reverse power sensor in the generator reverse power coupler, are then subtracted from the previously measured generator output power to give a reliable value for the microwave power absorbed in the cavity under the experimental conditions.

The discharge chamber pressure is measured during experimentation by a mechanical gauge and a fast response transducer, which are both connected to the upstream end of the discharge tube. The propellant mass flowrates in the two inlet channels are measured and controlled by mass flow controllers, which are insensitive to the pressure in the discharge tube. By making chamber pressure measurements under constant experimental conditions with a discharge present and then making them again under unchanged flow conditions with all power removed and the apparatus cooled to ambient temperatures, a hot-to-cold pressure ratio is obtained. From this the thrust and Isp during the discharge-on operation may be estimated [17], using the known propellant mass flowrate. With the power absorbed in the discharge known, the hot-to-cold pressure ratio also gives an estimate of the thruster thermal efficiency, affording a comparison with that calculated from the calorimetry measurements.

A two-color optical pyrometer will be employed to observe and measure the temperature of the interior of the throat/nozzle structure from an opening in the cryoliner target of the vacuum facility. A narrow bandpass filter on the pyrometer allows eliminating most of the interference from the plasma radiation of the exhaust plume, through which the instrument must look to observe the throat and nozzle surfaces. With internal calibration via a tungsten calibration lamp, temperature measurements with an accuracy of ($\pm$)50 K are feasible. Another useful application of optical pyrometry is in observing, through the cavity viewport, the opaque sidewalls of the high temperature discharge tubes employed during high power testing, to determine the plasma discharge location, volume, and characteristics.

Optical emission spectroscopy will be performed in the initial experiments in which the plasma discharge can be directly viewed to provide data from which the electron temperatures and densities in the plasmas can be extracted [9], [12]. More sensitive optical absorption spectroscopy will also be attempted across a cross section of the exhaust beam to measure its plasma and excitation properties and determine specie concentrations in the beam.

More elaborate diagnostics are planned in subsequent MET testing, based on the results from the initial measurements. These diagnostics are anticipated to include direct measurements of the throat/nozzle temperatures, the magnetic field during thruster testing, the plasma streaming velocity in the exhaust beam, and the thrust produced.

C. Results

At the time of this writing (May, 1991), only preliminary testing of components of the MET experimental apparatus has been completed. Results of these tests are summarized in this section.

The peak-to-peak ripple on the microwave generator output signal was measured at nominal power levels of 15, 22.5, and 27.5 kW, with the microwave circuit configured as described for the MET testing except for the use of a water load to simulate the cavity and its load. Prior to the ripple measurements, the three output phase voltages of the line regulator supplying 440 VAC power to the generator were balanced to minimize the 120 Hz ripple observed on the generator output signal. The ripple was measured on an oscilloscope with the probe placed across a 5-Ω resistor in the magnetron anode circuit. The observed ripple has both 120 and 720 Hz components (because of the full-wave rectified output circuit of the plate transformer) and the measured ripple was taken as the maximum peak-to-peak amplitude of the combined ac components. This was then divided by the median dc voltage of the signal, as ratioed up to correspond to a 30 kW output level, to get a percent full-scale ripple. The average values obtained were 1.82% at 15 kW, 2.37% at 22.5 kW, and 2.71% at 27.5 kW.

The operation of the phase shifter-tuner in adjusting and controlling the power applied to the cavity was also tested at nominal generator output levels of 15, 22.5, and 27.5 kW, again with a water load simulating the cavity and its load. The water load was instrumented for calorimetric measurements. The results of the testing are presented in Table I. At each nominal power level, the same procedure was followed to simulate a MET startup and power level increase to the maximum power available. The steps in this procedure are: 1) adjusting the phase shifter-tuner cranks for the minimum power transmitted to the cavity water load; 2) adjusting only the phase shifter crank to raise the power level transmitted to the cavity water load to a typical discharge starting level of 280–290 W; 3) continuing to adjust only the phase shifter crank to raise the power level at the cavity water load to the highest possible value; 4) adjusting first the tuner crank and then the phase shifter crank to obtain simultaneously the lowest possible power in the ballast water load and the highest possible power in the cavity water load; and 5) readjusting only the phase shifter crank to minimize the reflected power read by the generator reflected power sensor.

In Table I the nominal generator power is that read from a panel meter on the generator, which is wired to the magnetron anode circuit. The nominal phase shift is obtained

TABLE I
PHASE SHIFTER-TUNER POWER MANIPULATION TESTING

Step	Condition—See Text	Nominal Generator Power (kW)	Nominal Phase Shift (°)	Power to Cavity		Generator Reflected Power (kW)	Power to Ballast Water Load (kW)	Total Generator Power (kW)
				Directional Coupler (kW)	Water Load (kW)			
1.	Min. power to cavity load	26.4	−70	.00003	0.15	0.51	26.1	27.3
		22.5	−65	<.00007	0.15	0.38	23.2	24.3
		15.0	−80	<.00007	0.00	0.18	16.9	17.6
2.	Starting condtion	27.0	−90	0.29	0.29	0.41	26.7	28.0
		22.5	−90	0.28	0.29	0.40	23.0	24.2
		15.0	−110	0.28	0.29	0.20	16.3	17.2
3.	Max. power, phase shifter only	27.8	+70	10.1	9.8	0.43	18.7	29.6
		22.5	+65	7.8	7.8	0.48	16.4	25.2
		15.0	+60	5.8	5.9	0.19	10.9	17.5
4.	Max. power	27.3	0	28.8	29.0	0.60	0.3	30.7
		22.5	0	24.4	24.1	0.46	0.3	25.7
		15.0	0	16.6	16.5	0.18	0.3	17.7
5.	Max. power w/min. reflected power	27.1	+55	27.7	27.4	0.05	0.3	28.6
		22.5	+55	23.4	23.5	0.02	0.3	24.7
		15.0	+60	16.2	16.1	0.00	0.3	17.2

from the phase shifter crank position, based on calibration data. The power to the cavity is measured both by the forward power sensor of the dual directional coupler and by the cavity water load calorimetry. The total generator power is taken as the sum of the calorimetric measurements from the two water loads and the 3-port circulator, plus the reflected power read by the generator sensor. (The nominal generator power was held constant for the readings at 15 and 22.5 kW, but it fluctuated somewhat for the 27.5 kW readings because the power level control was left at its maximum value for these readings. The approximately 2 kW discrepancy between the nominal and total generator power values is attributed to calibration errors in the former.)

The trends in the Table I data are the same at all three power levels. Even at the highest power level, a combination of phase shifter-tuner crank positions can always be found, with a phase shift of about −70 degrees, to eliminate all power transmission to the cavity. (For these very lowest cavity power readings, the dual directional coupler readings are much more accurate than the calorimetric readings.) Changing the phase shift by about 25 degrees achieves the starting power level. The maximum cavity power level attainable by only changing the phase shift requires a further change of about 200 degrees, through (±)180 degrees. Adjusting the tuning crank as well then allows raising the cavity power level to the maximum value available, which is about three times as high. This maximum occurs for a phase shift of zero degrees, but the cavity power is found to be quite insensitive to the phase shift at maximum power. A further phase shift change of about 55 degrees then reduces the power reflected back to the generator to a minimum level, which is less than 0.2% of the total generator power. At the maximum cavity power conditions, the Table I data show that the microwave circuit transmits 94–95% of the total generator output power to the cavity, with the loss to the ballast water load always being less than 2%.

Pumping tests have been performed in the vacuum facility to determine its capacity for pumping the three propellant gases to be investigated in the MET testing. The tests were conducted with the diffusion pumps both on and off, as well as with various configurations of LN2 cryocooling in the tank. The maximum sustainable pumping capacities found with the diffusion pumps on and off are presented in Table II. The capacities with the diffusion pumps off are all well above the highest flowrates anticipated for near-term testing (50 000 sccm). The vacuum tank pressure under these conditions ranged from 55 Pa (0.4 Torr) for nitrogen to 200 Pa (1.5 Torr) for hydrogen, in all cases well over 1000 times lower than the anticipated discharge chamber pressures. Facility back pressure effects are therefore not expected to be a problem during the high flow testing.

As seen from Table II, the pumping capacities with the diffusion pumps on are about a factor of 10 lower than with the pumps off. The capacities with the diffusion pumps on are still substantial and allow testing at reduced facility back pressures of about 0.3 Pa (2 mTorr), in the event that the back pressure effects with the pumps off are significant. It should also be noted that the vacuum facility pressures are expected to be higher for comparable flowrates during the MET testing than those observed during the pumping tests because of the high temperatures of the exhausted propellant gases. This effect will reduce the actual pumping capacities during such testing below the values in Table II.

D. Planned Tests

The tests planned in the initial phases of the MET experimentation are as follows:

1) sweep generator characterization of the cavity modes

TABLE II
VACUUM FACILITY PUMPING CAPACITIES

Propellant Gas	Maximum Pumping Capacity (sccm), Diffusion Pumps	
	On	Off
Nitrogen	—[1]	101,000
Helium	17,200	198,000
Hydrogen	22,300	210,000

[1]No data comparable to that for helium and hydrogen available.

with the cavity empty and, alternatively, with the discharge chamber water-filled;

2) system testing to full power with the discharge chamber water-filled, verifying the power increase procedure and characterizing the magnetic nozzle field effects on the cavity operation;

3) low power testing on nitrogen at low pressure without the throat/nozzle structure installed, with characterization of magnetic nozzle effects;

4) low-medium power testing on nitrogen with the throat/nozzle structure installed and the magnetic nozzle in operation, using initially a quartz discharge tube and subsequently a high temperature (opaque) discharge tube;

5) testing on helium and then on hydrogen as in 3) and 4);

6) high power, high temperature testing on nitrogen with the magnetic nozzle in operation;

7) testing on helium and then on hydrogen as in 6).

This testing sequence will characterize the effects of the magnetic nozzle, the applied power, the discharge chamber pressure, different propellants, and flow injection variations on the MET performance, and it will provide a basis on which to define advanced, high power testing of the thruster concept to develop it as a practical spacecraft propulsion system.

IV. CONCLUSIONS

The microwave electrothermal thruster (MET) is an attractive advanced propulsion concept for medium to high power (30–200 kW) primary spacecraft propulsion. The potential performance of the MET on hydrogen propellant has been modelled with a two-dimensional kinetics (TDK) computer code. Operation of the thruster at a specific impulse of 2000 sec. is predicted to require an average discharge chamber temperature of about 6000 K at a chamber pressure of 1.0 MPa (10 atm.). These are performance goals set for the MET. The TDK computations do not take into account performance decrements due to thermal losses and wall effects, but when these are experimentally minimized, the MET performance is expected to approach the TDK predictions.

The MET concept is particularly suitable for use with a magnetic nozzle, in which a strong, solenoidal magnetic field is applied in the throat/nozzle region and extends into the plasma discharge region. The magnetic nozzle produces a powerful magnetic pressure on the discharge plasma which is directed radially inward, thereby compressing the plasma on the field axis. The beneficial effects of this include reducing wall heating and losses from the hot propellant species impinging on the walls, reducing frozen flow losses in the propellant exhausted from the nozzle, and controlling and stabilizing the location and shape of the discharge plasma on the field axis.

Apparatus is in final assembly with which to test the MET concept to power levels of 30 kW at a frequency of 915 MHz. The microwave generator and circuit have been installed and their performance characterized with a simulated cavity load. The generator and its magnetron circuitry have been optimized for minimum ripple on the output signal, and the peak-to-peak ripple has been measured at three power levels to be 2–3% of the full scale signal.

A phase shifter-tuner is incorporated in the microwave circuit by means of which the microwave power applied to the cavity can be continuously adjusted over the full range from the low power levels required for starting the MET to the maximum available from the generator. Thereby the need for altering the generator output power level during experimentation is eliminated. A procedure for accomplishing this power increase via the phase shifter-tuner controls has been verified and found to permit applying 0–95% of the generator output power to the cavity.

The resonant cavity of the apparatus has been assembled and the mechanical operation of its two internal tuning mechanisms verified. These mechanisms, which allow exactly matching the complex impedance of the discharge-loaded cavity to that of the source circuit, consist of an adjustable rear cavity endwall flange and an adjustable input power antenna. The cavity length may be adjusted to tune either the TM(011) or the TM(012) mode, both of which will be investigated.

Operation of the superconducting magnet providing the magnetic nozzle of the test apparatus has been verified, with a maximum on-axis field strength of 5.7 T achieved. Persistent mode operation, field reversal, and quench protection of the magnet have all been demonstrated. Pumping tests have been conducted with the vacuum facility employed with the MET apparatus to evaluate its pumping capacity for the three propellant gases to be tested: nitrogen, helium, and hydrogen. The facility was found capable of pumping, with the diffusion pumps off, considerably higher flowrates of each of the gases than required in the planned experiments. The facility pressures during the maximum flowrate pumping are low enough, of order 130 Pa (1 Torr), as not to pose significant interference with the MET testing or a significant effect on the measured thruster performance.

REFERENCES

[1] *Pioneering the Space Frontier*, U.S. National Commission on Space, Bantam Books, New York, 1986.

[2] J. E. Pollard, D. A. Lichtin, and R. B. Cohen, "RF discharge elec-

trothermal propulsion: Results from a lab-scale thruster," *AIAA Paper 87-2124*, June 1987.
[3] T. D. McCay and C. E. Dexter, "Chemical kinetic performance losses for a hydrogen laser thermal thruster," *J. Spacecraft*, vol. 24, pp. 372–376, July–Aug. 1987.
[4] J. Asmussen, R. Mallavarpu, J. Hamann, and H. Park, "The design of a microwave plasma cavity," *IEEE Proc.*, vol. 62, pp. 109–117, Jan. 1974.
[5] S. Whitehair and J. Asmussen, "Experiments and analysis of a compact microwave electrothermal thruster," *DGLR/AIAA/JSASS 20th Int. Electric Propulsion Conf.*, paper IEPC 88-101, Oct. 1988.
[6] V. M. Batenin, I. I. Klimovskii, and V. R. Khamraev, "Propagation of a microwave discharge in heavy atomic gases," *Soviet Physics JETP*, vol. 44, pp. 316–321, Aug. 1976.
[7] L. L. Frasch, "An experimental and theoretical study of a microwave cavity applicator loaded with lossy materials," Ph.D. dissertation, Michigan State University, E. Lansing, MI, 1987.
[8] Y. Arata, S. Miyake, and A. Kobayashi, "High power microwave discharge in atmospheric hydrogen gas flow," *J. Phys. Soc. Japan*, vol. 44, pp. 998–1003, Mar. 1978.
[9] M. C. Hawley, J. Asmussen, J. W. Filpus, S. Whitehair, C. Hoekstra, T. J. Morin, and R. Chapman, "Review of research and development on the microwave electrothermal thruster," *J. Prop. and Power*, vol. 5, pp. 703–712, Nov.–Dec. 1989.
[10] J. L. Power and R. A. Chapman, "Development of a high power microwave thruster, with a magnetic nozzle, for space applications," *NASA TM 102321*, Aug. 1989.
[11] G. R. Nickerson, D. E. Coats, A. L. Dang, S. S. Dunn, and H. Kehtarnavaz, "Two-dimensional kinetics (TDK) nozzle performance computer program"; Software and Engineering Associates, Inc., Carson City, NV, Mar. 1989.
[12] S. Haraburda, "Diagnostic evaluations of microwave generated helium and nitrogen plasma mixtures"; *AIAA Paper 90-2634*, July 1990.
[13] W. A. Herlan and D. M. Jassowski, "Microwave thruster development," *AIAA Paper 87-2123*, June 1987.
[14] S. S. Haraburda and M. C. Hawley, "Investigations of microwave plasmas (applications in electrothermal thruster systems)," *AIAA Paper 89-2378*, July 1989.
[15] F. M. Curran and T. W. Haag, "An extended life and performance test of a low-power arcjet," *AIAA Paper 88-3106*, July 1988.
[16] T. A. Keller, and G. A. Wise, "Experimental results of a 1500-cubic-feet unbaked ultrahigh vacuum system," in *High-Vacuum Technology, Testing, and Measurement Meeting, Compilation of Papers*, June 8–9, 1965, *NASA TM X-1268*, pp. 19–25, Aug. 1966.
[17] S. Whitehair, J. Asmussen, and S. Nakanishi, "Microwave electrothermal thruster performance in helium gas," *J. Prop. and Power*, vol. 3, pp. 136–144, Mar.–Apr. 1987.

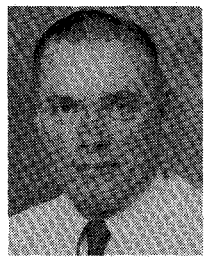

John L. Power received the B.S. degree from Yale University in 1956 and an M.S. degree from Princeton University in 1958. He did additional graduate work at Princeton during 1958–1961.

From 1961 to the present he has been employed at the NASA-Lewis Research Center in Cleveland, OH, as a Physicist and Aerospace Engineer. During the period from 1961 to 1971, he did research in the nuclear chemistry of cyclotron-produced radioisotopes and in nuclear reactor technology. He designed and operated an in-core experiment in the NASA-Plum Brook 60 MW research reactor to test the feasibility of a novel reactor control concept. From 1971 to the present, he has primarily been engaged in research and development in the field of electric propulsion. Much of this work has been in developing electrostatic ion thrusters for auxiliary propulsion applications on spacecraft. Specific areas of concentration include thruster durability, thruster operating control algorithms, thruster/spacecraft interactions, and thruster mission applications. He was Principal Investigator for the Ion Auxiliary Propulsion System (IAPS) flight test of two 8-cm diameter mercury ion thrusters on an Air Force mission scheduled for launch in 1986 but indefinitely postponed after the Shuttle Challenger accident. Since 1988 Mr. Power has been engaged in the experimental investigation of microwave electrothermal thrusters and the prediction of their performance.